nature structural biology

A structural model for actin-induced nucleotide release in myosin

Thomas F Reubold[1], Susanne Eschenburg[1], Andreas Becker[1,4], F Jon Kull[2] & Dietmar J Manstein[1,3]

Myosins are molecular motor proteins that harness the chemical energy stored in ATP to produce directed force along actin filaments. Complex communication pathways link the catalytic nucleotide-binding region, the structures responsible for force amplification and the actin-binding domain of myosin. We have crystallized the nucleotide-free motor domain of myosin II in a new conformation in which switch I and switch II, conserved loop structures involved in nucleotide binding, have moved away from the nucleotide-binding pocket. These movements are linked to rearrangements of the actin-binding region, which illuminate a previously unobserved communication pathway between the nucleotide-binding pocket and the actin-binding region, explain the reciprocal relationship between actin and nucleotide affinity and suggest a new mechanism for product release in myosin family motors.

Existing crystal structures of myosin show two major conformations in the nucleotide-binding pocket, 'closed' and 'open,' which are linked to the position of the force-generating lever arm being in an 'up' or 'down' position[1–7]. The closed conformation, which is the catalytically active state, is characterized by specific interactions of two loop regions, switch I and switch II, with the bound nucleotide. Switch II contains a conserved glycine residue whose amide nitrogen forms a hydrogen bond with the γ-phosphate in the closed conformation that is broken in the open conformation. Switch I contains a conserved sequence motif, SSR, in which the first serine forms a hydrogen bond with the γ-phosphate, if present, and the second serine coordinates the Mg^{2+} ion of the bound nucleotide in both open and closed states. The arginine residue is involved in a salt bridge with a conserved glutamate in switch II[6,8]. This salt bridge is formed in the closed conformation, but broken in the open state. As residues from switch I cover the phosphate-binding region, it has been postulated that myosin operates via a 'back-door' mechanism, with the γ-phosphate leaving the catalytic site through a tunnel that exists in the open state[9]. One difficulty with this model is that this escape route may be sterically blocked when myosin is bound to actin. Furthermore, the open state is thought to be linked to the lever arm being in the down, post-powerstroke state, but release of inorganic phosphate (P_i) is thought to occur before force generation. We have solved the X-ray structure of the nucleotide-free myosin II motor domain from *Dictyostelium discoideum* to a resolution of 1.9 Å. This new structure shows coordinated changes in the actin-binding region and the position of the lever arm, and, moreover, elucidates the mechanism of product release. In this new structure, the entire switch I region has moved away from the nucleotide-binding site, providing a large opening by which the P_i can leave the nucleotide-binding site via a 'trapdoor' rather than a 'back door.'

RESULTS

Nucleotide binding site

Comparing the nucleotide-binding site of the new crystal structure of the myosin II motor domain (**Fig. 1a**) with that in previously determined structures of myosin II in its closed (PDB entry 1VOM; **Fig. 1b**) and open (PDB entry 1MMA; **Fig. 1c**) conformations, the most striking difference lies in the position of switch I. In the new structure, the switch I region has moved ~8 Å away from its usual position. Unlike a recent structure of nucleotide-free myosin that shows switch I becoming disordered[10], the transition we observe maintains a well ordered switch I loop (**Fig. 1d**). Switch II is in the open position, as the glycine is not in a position that would support hydrogen bonding with the γ-phosphate. To standardize myosin's various conformational states, we will refer to this new conformation as switch I open, switch II open, or simply open/open (O/O). All previously determined structures containing nucleotide show switch I to be in the closed state, as defined by an interaction of the conserved switch I serine with the Mg^{2+} ion. Therefore, the old open, or near-rigor state will now be referred to as switch I closed, switch II open (closed/open or C/O). The old closed, or transition state, will be referred to as closed/closed (C/C).

The movement of switch I results in a major disruption of interactions that stabilize not only γ-phosphate binding, but also the coordination of the Mg^{2+} ion, and therefore ADP binding. In

[1]Abteilung Biophysik, Max-Planck Institut für medizinische Forschung, Jahnstr. 29, D-69120 Heidelberg, Germany. [2]Dartmouth College, Department of Chemistry, 6128 Burke Laboratory, Hanover, New Hampshire 03755, USA. [3]Institut für Biophysikalische Chemie, OE4350, Medizinische Hochschule Hannover, Carl-Neuberg-Str. 1, 30623 Hannover, Germany. [4]Present address: University of Kansas, Department of Medicinal Chemistry, 4040a Malott Hall, Lawrence, Kansas 66045, USA. Correspondence should be addressed to D.J.M. (Manstein@bpc.mh-hannover.de).

Published online 21 September 2003; doi:10.1038/nsb987

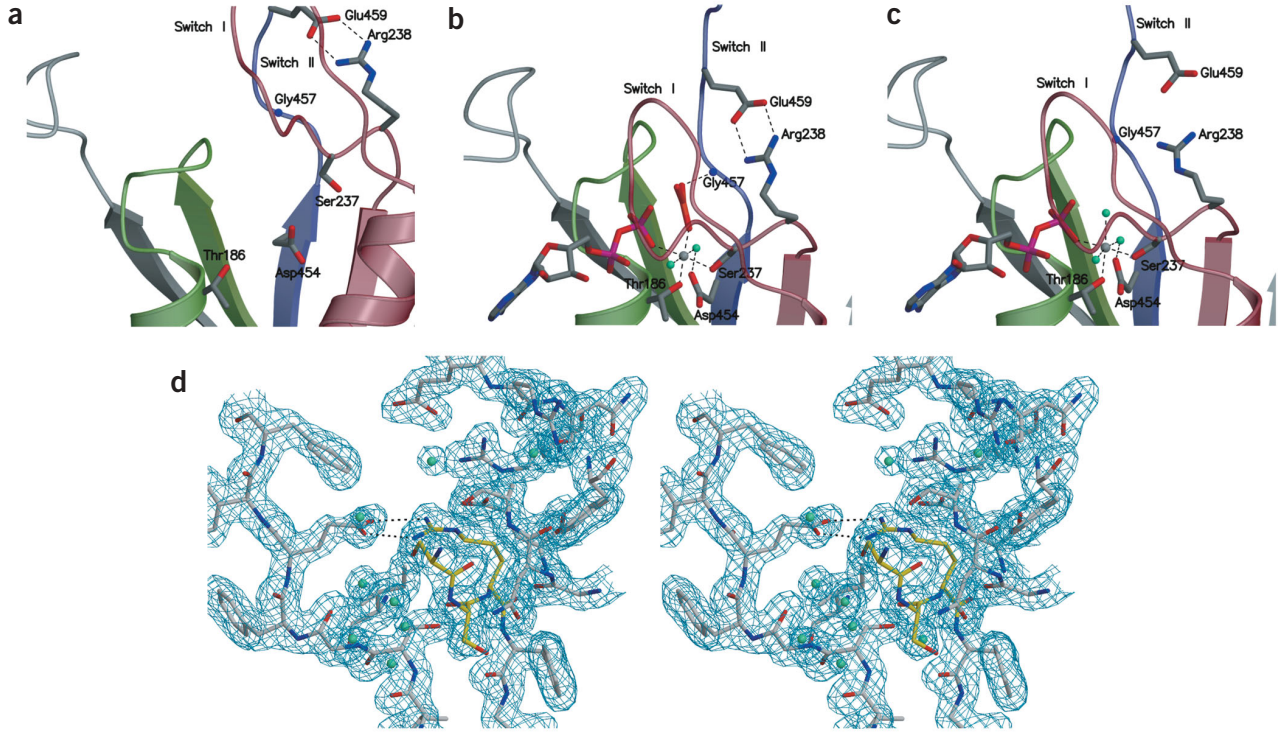

Figure 1 Three conformations of the myosin II nucleotide-binding pocket. (**a**) Nucleotide-free structure with both switch I (pink) and switch II (blue) in an open conformation. (**b**) Structural elements surrounding Mg-ADP-BeF_3 in a C/C complex. The P-loop β-strand and loop (green) coordinate the Mg^{2+} ion through Thr186. Switch I interacts directly with the nucleotide γ-phosphate (BeF_3 in this structure) via interactions with Ser236 (not shown) and indirectly through Mg^{2+}, which is coordinated by Ser237. Switch II interacts with the γ-phosphate directly via a hydrogen bond from Gly457 (blue sphere) and indirectly with the Mg^{2+} from Asp454 and a bridging water molecule (waters, cyan spheres). Binding interactions, dashed lines. (**c**) Structural elements surrounding Mg-ADP in a C/O complex. The P-loop β-strand and loop coordinate the Mg^{2+} ion through Thr186. Switch I has not moved and interacts with the nucleotide indirectly through Mg^{2+}, which is coordinated by Ser237. Switch II has moved ~5 Å away from the nucleotide-binding site, Gly457 no longer interacts with the nucleotide and the salt bridge is broken. Asp454 still interacts with the nucleotide via a bridging water molecule. (**d**) Representative electron density for a segment centered around the salt bridge that is formed by residues Arg238 and Glu459. Salt-bridge interaction, dotted lines; switch I motif, yellow. The $2F_o - F_c$ map is contoured at 1.0 σ. Water molecules, green spheres.

combination with switch II being in an open conformation, virtually all essential interactions with the nucleotide are lost. In the C/C and C/O structures, two conserved serines in switch I interact with the nucleotide, both directly when a γ-phosphate is present and indirectly via the Mg^{2+}. Switch II interacts directly with the γ-PO_4 in the C/C structure via glycine, and indirectly with aspartate, which binds the Mg^{2+} ion through a bridging water molecule. The major difference between the C/C and C/O structures is in the movement of switch II away from the nucleotide (**Fig. 1**). This removes the glycine and weakens the hydrogen bond from the aspartate residue. It also pulls the glutamate away, breaking the salt bridge. Very little change is observed in the switch I residues. In the new O/O structure, switch II has moved even farther away and switch I has moved back by ~8 Å, thereby removing both serines from the vicinity of the nucleotide. Furthermore, the remaining switch II interaction, between the aspartate and Mg^{2+} via a bridging water molecule, is also eliminated. The movements completely abolish any potential for interactions between the nucleotide γ-phosphate and the myosin, as well as almost all coordination, either direct or indirect, between the protein and the Mg^{2+} ion. Only one interaction could remain, between a threonine in the phosphate-binding P-loop of the protein and the Mg^{2+} ion. In effect the combined movements of switch I and II greatly facilitate the release of P_i and Mg^{2+}-ADP.

Actin binding region

The movement of switch I is linked to a large change in the relative position of the 50K domain and the rest of the motor domain, including the P-loop, N terminus, and converter domain (**Fig. 2**). In relation to a superposition of the P-loops, the 50K domain, which consists of an upper and lower subdomain (**Fig. 2a**), undergoes a rotation that positions elements of the actin-binding region between 12 Å and 20 Å away from their positions in the previously determined crystal structures (**Fig. 2b**). Although rotation of both the upper and lower 50K domains occurs, the relative rotation is not identical, and the distance between the tip of the cardiomyopathy loop of the upper 50K domain and the tip of the loop in the helix-turn-helix motif of the lower 50K domain increases substantially, from 16.1 Å in the C/O state to 20.4 Å in the C/C state and 26.0 Å in this new O/O state (**Fig. 2c**). Despite these differences, there is not any substantial gain or loss of interactions across the 50K cleft. Instead, the differences are due to a rearrangement of the central β-sheet beyond the P-loop β-strand. The trajectories of the three edge β-strands have changed in such a way as to introduce the observed rotation of the upper and lower 50K domains (**Fig. 2d**). This type of β-sheet rearrangement has not been observed so far in motor proteins, but such rearrangements have been described for Arf family G-proteins as they cycle between GTP-bound and GDP-

bound states[11]. G-proteins and motor proteins share many structural features including the P-loop, switch regions and topology of the central β-sheet[12–15], and it has been pointed out that common features are also reflected in shared kinetic and thermodynamic principles[15]. The reason why the β-sheet rearrangements involve a change in the register of hydrogen bonds in some G-proteins but not in myosin may reflect their different cellular functions as molecular switches and motors. We believe that crystal packing has trapped a conformation in which the upper and lower actin-binding regions have been repositioned in a way that starts to resemble the rigor conformation. However, there is growing evidence that the 50K cleft closes upon tight binding to actin and formation of the rigor complex[16–18]. In the absence of actin, we do not expect the cleft of a conventional myosin to be closed, and therefore place this structure on the path to the rigor state, but not yet in the full rigor conformation.

Lever arm

Superposition of the 50K domains of this structure with those of the C/O and C/C structures reveals that the lever arm is in the down position, similar to that observed for previously determined C/O structures with switch II in the open conformation. Even though the salt bridge between switch I and switch II is formed, as in the C/C structures, the simultaneous movement of the upper and lower 50K domains relieves the steric constraints, causing the helix following switch II to kink; this is linked to rotation of the converter domain and lever arm in the C/C structures. Therefore, the tight correlation of an open switch II with the lever arm in the down position is maintained in this structure.

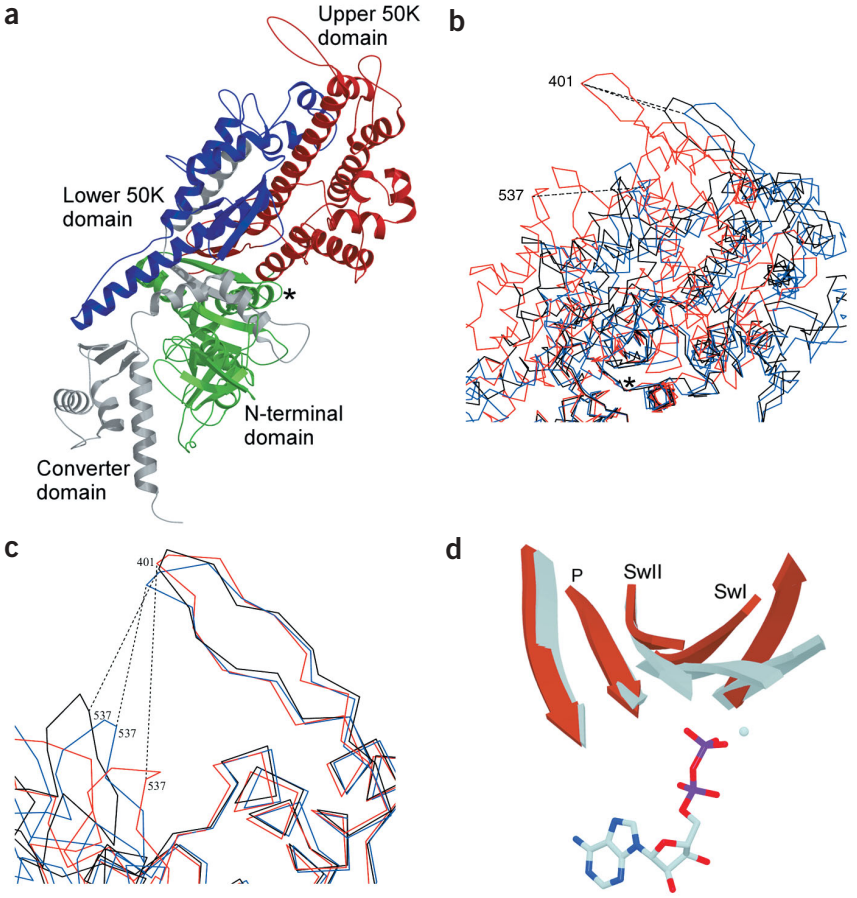

Figure 2 Global conformational changes in the O/O conformation of myosin II. (**a**) Ribbon diagram of the nucleotide-free structure indicating the subdomains of the myosin motor. (**b**) P-loop superposition of the three myosin conformations shows the movement of the 50K domain with respect to the rest of the molecule. C/C, blue; C/O, black; O/O, red. Orientation as in **a**. Dashed lines indicate distance between identical residues in the three conformations (Gly401 in the cardiomyopathy loop and Asn537 in the helix-turn-helix motif). (**c**) Superposition of the upper 50K domains reveals large differences with respect to the position of the lower 50K domain. (**d**) Changes in the orientation of three edge β-strands results in the global changes shown in **b** and **c**. P-loop superposition was used with a similar orientation to that in **b**. Five core strands are shown for the C/O (gray) and O/O (red) conformations. The left-most two strands remain closely overlapping over their entire lengths, whereas the three strands on the right diverge substantially at the top of the sheet while remaining in the same position at the bottom. P, strand preceding the P-loop; SwII, strand preceding the switch-II loop; SwI, strand following switch I. The ADP is shown from the C/O structure for reference. The asterisks in **a** and **b** mark the P-loop.

DISCUSSION

Based on these results, we present a potential scheme for the myosin cycle (**Fig. 3**). In the C/C transition-state structure both switch I and switch II are in the closed position, phosphate release is blocked and the lever arm is in the up position. Hydrolysis results in cleavage of the phosphoanhydride bond between the β- and γ-phosphates and simultaneously leads to the destabilization of the C/C state. The equilibrium between C/C and O/C is further shifted toward the O/C conformation by actin binding. Weak association with actin induces a rearrangement of the actin-binding interface, resulting in the opening of switch I. The opening of switch I breaks the salt bridge between Arg238 and Glu459, and accelerates P_i release through a newly formed 'trapdoor.' Loss of P_i disrupts the hydrogen bond between the switch II glycine and the γ-phosphate, thereby allowing switch II to open, leading to ADP release, swinging of the lever arm, force generation and formation of a tightly bound rigor conformation. This conformation would be similar to the O/O structure described in this paper, but with the cleft between the upper and lower 50K domains possibly more closed. Binding of ATP via interactions with the P-loop triggers the closing of switch I and the breaking of the salt bridge between switch I and switch II. These ATP-induced changes of the nucleotide-binding site are communicated via the three edge β-strands to the actin-binding residues of the upper and lower 50K domains. The resulting disruption of the tight actin-binding interface allows switch II to move in toward the γ-phosphate, repositioning the lever arm and restoring the C/C, hydrolysis-competent conformation.

The salt bridge between switch I and switch II seems to help in orienting the critical catalytic residues from switch I and switch II when myosin is bound to actin or ATP[10]. It provides an energy minimum for stabilizing the conformations that represent the catalytically

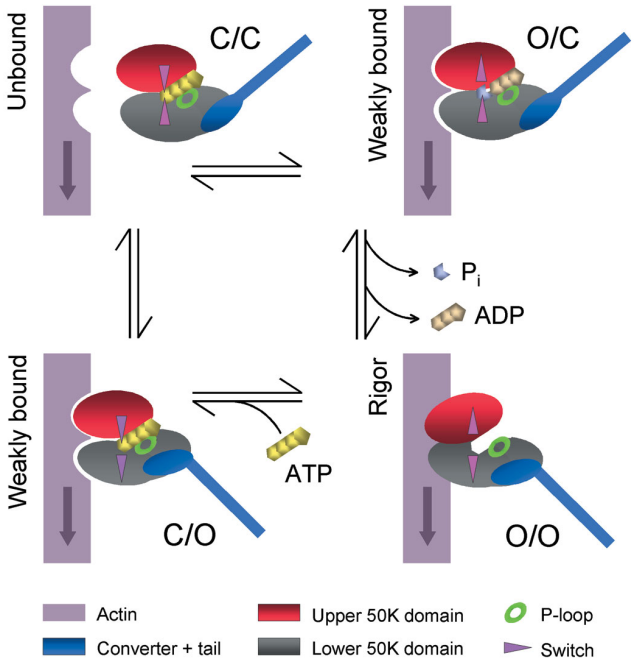

Figure 3 Structural model for the actin-activated myosin II ATPase cycle.

active (C/C) state and the rigor state (O/O). When broken, the salt-bridge residues are placed so as to assist in the catalytic mechanism by either charge-charge attraction or charge-charge repulsion. In C/C, both Arg238 and Glu459 are ~5 Å from the γ-phosphate, and they are in a salt bridge, effectively canceling their charge. This role of the salt bridge is in good agreement with the experimental results of mutant studies[8,19]. In C/O structures, Glu459 is observed to be positioned 8 Å from the γ-phosphate. Arg238 is only 5 Å from the γ-phosphate and could thus support ATP binding via charge-charge interactions during the formation of the C/O conformation. Inversion of the orientation of the salt-bridge residues in motor domain construct M765-IS does indeed result in a 2,500-fold higher K_m for ATP and a 15-fold reduction in the rate of ATP binding to myosin. The finding that the second-order rate constants for ADP binding are almost identical for wild-type and myosin-IS supports the notion that the interaction with the salt-bridge residue specifically affects the γ-phosphate[8]. In addition to the function of the salt bridge in stabilizing ATP and actin binding, the salt-bridge residues also seem to have a role in facilitating P_i release. During the transition from the C/C conformation to the hypothetical O/C conformation, switch I moves away from the ATP-binding site, leaving the switch II glutamate ~5 Å away from the γ-phosphate. Switch I is in an open conformation, where it is ~10 Å away from the γ-phosphate site. The charge repulsion between Glu459 and P_i should thus help to drive the release of the hydrolysis product.

The model presented above proposes four primary conformations for myosin, which can be distinguished by the position (open or closed) of the switch I and switch II regions. Previously determined structures describe the C/C and C/O states, and this structure represents a third conformation, O/O. The fourth state, O/C, remains to be visualized for myosin; however, a conformation resembling this state has been observed for Kif1A, a member of the structurally related kinesin superfamily of motors[20]. Although the switch II glycine in the Kif1A structure has not moved toward the nucleotide far enough to form a hydrogen bond, it is more closed than in other kinesin structures. As all kinesin structures determined to date show switch I in the open state, the partially closed Kif1A structure suggests that switch II can move independently of switch I in kinesins, and may do the same in myosins. These similarities lend more evidence to the idea that both types of motor proteins use the same structural mechanisms to initiate force generation, and that conformational states observed in one motor family may presage yet unobserved states in the other family.

METHODS

Protein expression and purification. Residues 2–765 of the catalytic domain of *Dictyostelium* myosin II were fused to the N terminus of the rat dynamin1 GTPase domain. We use the myosin fusion system to facilitate the expression, purification and crystallization of proteins and protein domains[6,21]. The system relies on the functional integrity of the myosin motor domain, as the purification of the fusion protein is based on the ATP-dependent binding of the myosin part of the fusion to actin. The structure of the rat dynamin1 GTPase domain will be published elsewhere. The N-terminally His-tagged 120-kDa fusion protein was expressed in *Dictyostelium* AX3-ORF$^+$ and purified as described earlier for the myosin part alone[22,23]. In brief, cells were lysed with 0.5% (v/v) Triton TX-100 in 20 cell volumes of buffer containing 50 mM Tris, pH 8.0, 2 mM EDTA, 0.2 mM EGTA, 2 mM DTT, 5 mM benzamidine and protease inhibitors. The fusion protein was pelleted as actin rigor complex for 1 h at 30,000*g* and then resolubilized by homogenization in two cell volumes of extraction buffer containing 50 mM HEPES, pH 7.3, 30 mM K-acetate, 300 mM NaCl, 14 mM Mg-acetate, 7 mM β-mercaptoethanol, 10 mM ATP, 2 mM GTP and protease inhibitors. After centrifugation for 20 min at 20,000*g* the supernatant was applied to an XK16 column (Amersham Pharmacia) packed with Ni-NTA resin (Qiagen). The column was washed with three different buffers (50 mM HEPES, pH 7.3, 300 mM K-acetate; 50 mM HEPES, pH 7.3, 30 mM K-acetate; 30 mM imidazole, pH 7.3). The fusion protein was eluted with a gradient from 50 to 500 mM imidazole over 5 column volumes. Peak fractions were pooled and dialyzed against storage buffer containing 50 mM Tris, pH 8.0, 1 mM $MgCl_2$, 5 mM DTT, 3% (w/v) sucrose. The dialyzed fusion protein was further purified by size-exclusion chromatography using a Superdex 200 (Amersham Pharmacia) gel filtration column equilibrated with storage buffer. Peak fractions were concentrated to 18 mg ml^{-1} using 20 ml VIVASPIN concentration devices (VIVASCIENCE) with a cutoff of 50 kDa, and subsequently flash frozen in liquid nitrogen and stored at –80 °C. The purified fusion protein moved actin filaments *in vitro* with a velocity of 100 nm s^{-1} at 30 °C.

Protein crystallization. Crystals were grown by the hanging-drop method at 4 °C using 11% (w/v) PEG-8000, 140 mM NaCl, 1 mM EGTA, 5 mM $MgCl_2$, 5 mM DTT and 2% (v/v) 2-methyl-2,4-pentanediol (MPD) as reservoir solution. Droplets were mixed from equal volumes of reservoir solution and protein solution (18 mg ml^{-1}). Crystals typically grew within 3–5 d to a size of ~500 × 120 × 120 µm. For cryoprotection crystals were transferred into a drop of 20 µl reservoir solution with 13% (w/v) PEG-8000, then 20 µl of the same solution containing 50% (v/v) glycerol were added stepwise. For derivatization a crystal was soaked for 12 h in reservoir solution with 13% (w/v) PEG-8000 containing 0.1 mM methyl mercury chloride. Cryoprotection was carried out as described using cryoprotectant containing 0.1 mM of methyl mercury chloride. Crystals were flash frozen in liquid propane and transferred to liquid nitrogen for storage.

Data collection and processing. Native data were collected at 100 K on an ADSC CCD detector using synchrotron radiation (0.93927 Å) at beamline ID 14-4 (European Synchrotron Radiation Facility, Grenoble, France). A full data set to 1.9-Å resolution has been obtained from two crystals. Heavy-atom data were collected to 2.3 Å from a single crystal at 100 K on a MAR345 image plate detector using CuK radiation from a rotating anode (generator: GX-18, Elliott/Enraf-Nonius) operated at 35 kV and 50 mA. Native and derivative data were processed with XDS[24] and scaled with XSCALE[24].

Table 1 Data collection, structure solution and refinement statistics

Data collection		
Crystal	Native	Derivative
Space group	$P2_12_12_1$	$P2_12_12_1$
Unit cell dimensions		
a (Å)	57.4	57.4
b (Å)	127.0	127.0
c (Å)	160.8	160.8
$\alpha = \beta = \gamma$	90	90
Molecules/asymmetric unit	1	1
Resolution range[a]	20–1.9 (2.0–1.9)	20–2.25 (2.3–2.25)
Measured reflections[a]	1,215,184 (104,933)	512,629 (27,710)
Unique reflections[a]	92,665 (12,446)	56,081 (3,447)
Completeness[a] (%)	99.1 (94.9)	98.5 (96.0)
R_{sym}[a,b] (%)	9.8 (17.1)	7.5 (27.7)
Phasing		
Resolution range (Å)	15.0–2.30	
Number of sites	6	
Phasing power		
Isomorphous	1.5	
Anomalous	1.2	
Figure of merit	0.52	
Refinement		
Protein atoms	8,507	
Solvent molecules	754	
R.m.s. deviation from ideal values		
Bond length (Å)	0.017	
Bond angle (°)	1.69	
R_{cryst}[c] (%)	18.5	
R_{free}[d] (%)	22.4	

[a]Values in parentheses are for highest-resolution shell [b]$R_{sym} = \Sigma_{hkl}\Sigma_i |I_{hkl,i} - \langle I_{hkl}\rangle| / \Sigma_{hkl,i} |I_{hkl}$ where *h* are unique reflection indices. [c]$R_{cryst} = 100 \times \Sigma||F_o| - |F_c|| / \Sigma|F_o|$ where F_o and F_c are observed and calculated structure factor amplitudes. [d]R_{free} and R_{cryst} were calculated for randomly chosen reflections, which were excluded from the refinement (2.5% of the unique reflections)

Phasing, model building and refinement. The structure of the fusion protein has been solved by the SIRAS method using a single mercury derivative. All calculations for phasing and refinement were done with the program package CNS[25]. Building of the initial model and all manual adjustments during structure refinement were done with the program O[26]. Refinement was carried out using data to highest resolution with no σ cutoff applied. Solvent molecules were automatically picked as implemented in CNS and checked manually. Statistics of data collection, structure solution and refinement are summarized in **Table 1**. **Figure 1a** was prepared using BobScript[27] and Raster3D[28]; **Figures 1b–d** and **2a–d** were produced using MolScript[29] and Raster3D[28].

Coordinates. The coordinates of the nucleotide-free myosin II motor domain have been deposited in the Protein Data Bank (accession code 1Q5G).

ACKNOWLEDGMENTS
We thank W. Kabsch for crystallographic advice, S. Zimmermann and A. Scherer for excellent technical assistance, S. Fujita-Becker for *in vitro* motility analysis and K.C. Holmes for helpful comments, discussions and continuous support. The work was supported by Molecular Motors project grants from the Deutsche Forschungsgemeinschaft.

COMPETING INTERESTS STATEMENT
The authors declare that they have no competing financial interests.

Received 30 May; accepted 7 August 2003
Published online at http://www.nature.com/naturestructuralbiology/

1. Rayment, I. *et al.* Three-dimensional structure of myosin subfragment-1: a molecular motor. *Science* **261**, 50–58 (1993).
2. Fisher, A.J. *et al.* X-ray structures of the myosin motor domain of *Dictyostelium discoideum* complexed with MgADP.BeF_x and MgADP.AlF_4^-. *Biochemistry* **34**, 8960–8972 (1995).
3. Smith, C.A. & Rayment, I. X-ray structure of the magnesium(II).ADP.vanadate complex of the *Dictyostelium discoideum* myosin motor domain to 1.9 Å resolution. *Biochemistry* **35**, 5404–5417 (1996).
4. Dominguez, R., Freyzon, Y., Trybus, K.M. & Cohen, C. Crystal structure of a vertebrate smooth muscle myosin motor domain and its complex with the essential light chain: visualization of the pre-power stroke state. *Cell* **94**, 559–571 (1998).
5. Houdusse, A., Kalabokis, V.N., Himmel, D., Szent-Gyorgyi, A.G. & Cohen, C. Atomic structure of scallop myosin subfragment S1 complexed with MgADP: a novel conformation of the myosin head. *Cell* **97**, 459–470 (1999).
6. Kliche, W., Fujita-Becker, S., Kollmar, M., Manstein, D.J. & Kull, F.J. Structure of a genetically engineered molecular motor. *EMBO J.* **20**, 40–46 (2001).
7. Kollmar, M., Dürrwang, U., Kliche, W., Manstein, D.J. & Kull, F.J. Crystal structure of the motor domain of a class-I myosin. *EMBO J.* **21**, 2517–2525 (2002).
8. Furch, M., Fujita-Becker, S., Geeves, M.A., Holmes, K.C. & Manstein, D.J. Role of the salt-bridge between switch-1 and switch-2 of *Dictyostelium* myosin. *J. Mol. Biol.* **290**, 797–809 (1999).
9. Yount, R.G., Lawson, D. & Rayment, I. Is myosin a 'back door' enzyme? *Biophys. J.* **68**, 47S–49S (1995).
10. Himmel, D.M. *et al.* Crystallographic findings on the internally uncoupled and near-rigor states of myosin: further insights into the mechanics of the motor. *Proc. Natl. Acad. Sci. USA* **99**, 12645–12650 (2002).
11. Pasqualato, S., Renault, L. & Cherfils, J. Arf, Arl, Arp and Sar proteins: a family of GTP-binding proteins with a structural device for 'front-back' communication. *EMBO Rep.* **3**, 1035–1041 (2002).
12. Smith, C.A. & Rayment, I. Active site comparisons highlight structural similarities between myosin and other P-loop proteins. *Biophys. J.* **70**, 1590–1602 (1996).
13. Vale, R.D. Switches, latches, and amplifiers: common themes of G proteins and molecular motors. *J. Cell Biol.* **135**, 291–302 (1996).
14. Kull, F.J., Vale, R.D. & Fletterick, R.J. The case for a common ancestor: kinesin and myosin motor proteins and G proteins. *J. Muscle Res. Cell Motil.* **19**, 877–886 (1998).
15. Goody, R.S. & Hofmann-Goody, W. Exchange factors, effectors, GAPs and motor proteins: common thermodynamic and kinetic principles for different functions. *Eur. Biophys. J.* **31**, 268–274 (2002).
16. Volkmann, N. *et al.* Evidence for cleft closure in actomyosin upon ADP release. *Nat. Struct. Biol.* **7**, 1147–1155 (2000).
17. Volkmann, N. *et al.* Myosin isoforms show unique conformations in the actin-bound state. *Proc. Natl. Acad. Sci. USA* **6**, 3227–3232 (2003).
18. Yengo, C.M., De La Cruz, E.M., Chrin, L.R., Gaffney, D.P. 2nd & Berger, C.L. Actin-induced closure of the actin-binding cleft of smooth muscle myosin. *J. Biol. Chem.* **277**, 24114–24119 (2002).
19. Friedman, A.L., Geeves, M.A., Manstein, D.J. & Spudich, J.A. Kinetic characterization of myosin head fragments with long-lived myosin-ATP states. *Biochemistry* **37**, 9679–9687 (1998).
20. Kikkawa, M. *et al.* Switch-based mechanism of kinesin motors. *Nature* **411**, 439–445 (2001).
21. Niemann, H.H., Knetsch, M.L., Scherer, A., Manstein, D.J. & Kull, F.J. Crystal structure of a dynamin GTPase domain in both nucleotide-free and GDP-bound forms. *EMBO J.* **20**, 5813–5821 (2001).
22. Manstein, D.J., Schuster, H.P., Morandini, P. & Hunt, D.M. Cloning vectors for the production of proteins in *Dictyostelium discoideum*. *Gene* **162**, 129–134 (1995).
23. Manstein, D.J. & Hunt, D.M. Overexpression of myosin motor domains in *Dictyostelium*: screening of transformants and purification of the affinity tagged protein. *J. Mus. Res. Cell Motil.* **16**, 325–332 (1995).
24. Kabsch, W. Automatic processing of rotation diffraction data from crystals of initially unknown symmetry and cell constants. *J. Appl. Cryst.* **26**, 795–800 (1993).
25. Brunger, A.T., *et al.* Crystallography & NMR system: a new software suite for macromolecular structure determination. *Acta Crystallogr. D* **54**, 905–921 (1998).
26. Jones, T.A., Zou, J.Y., Cowan, S.W. and Kjeldgaard, M. Improved methods for binding protein models in electron density maps and the location of errors in these models. *Acta Crystallogr. A* **47**, 110–119 (1991).
27. Esnouf, R.M. An extensively modified version of MolScript that includes greatly enhanced coloring capabilities. *J. Mol. Graph. Model* **2**, 132–134 (1997).
28. Merritt, E.A. and Bacon, D.J. Raster3D: photorealistic molecular graphics. *Methods Enzymol.* **277**, 505–524 (1997).
29. Kraulis, P.J. MOLSCRIPT: a program to produce both detailed and schematic plots of protein structures. *J. Appl. Crystallogr.* **24**, 946–950 (1991).